Ras Mediates Effector Pathways Responsible for Pre-B Cell Survival, Which Is Essential for the Developmental Progression to the Late Pre-B Cell Stage

By Hitoshi Nagaoka,* Yoshimasa Takahashi,* Reiko Hayashi,‖ Tohru Nakamura,*¶ Kumiko Ishii,* Junichiro Matsuda,‡ Atsuo Ogura,‡ Yumiko Shirakata,** Hajime Karasuyama,‡‡ Tetsuo Sudo,§§ Shin-Ichi Nishikawa,‖‖ Takeshi Tsubata,¶¶ Tsuguo Mizuochi,¶ Toshihiko Asano,§ Hitoshi Sakano,‖ and Toshitada Takemori*

*From the *Department of Immunology, the ‡Department of Veterinary Science, and the §Division of Experimental Animal Research, National Institute of Infectious Diseases, Tokyo 162-8640, Japan; the ‖Department of Biophysics and Biochemistry, Graduate School of Science, University of Tokyo, Tokyo 113-0033, Japan; the ¶Laboratory of Biomedical Chemistry, Department of Applied Chemistry, Tokai University, Kanagawa 259-1292, Japan; the **Department of Gene Research, The Cancer Institute, Japanese Foundation for Cancer Research, Tokyo 170-8455, Japan; the ‡‡Department of Immunology, The Tokyo Metropolitan Institute of Medical Science, Tokyo 113-8613, Japan; the §§Toray Basic Research Laboratories, Kanagawa-ken 259-1192, Japan; the ‖‖Department of Molecular Genetics, Graduate School of Medicine, Kyoto University, Kyoto 606-8507, Japan; and the ¶¶Department of Immunology, Medical Research Institute, Tokyo Medical and Dental University, Tokyo 113-8510, Japan*

Abstract

Ras is essential for the transition from early B cell precursors to the pro-B stage, and is considered to be involved in the signal cascade mediated by pre-B cell antigen receptors. To examine the role of $p21^{ras}$ in the late stage of B cell differentiation, we established transgenic mice (TG) expressing a dominant-inhibitory mutant of *Ha-ras* (Asn-17 *Ha-ras*) in B lineage cells at high levels after the early B cell precursor stage. Expression of $p21^{Asn\text{-}17\ Ha\text{-}ras}$ was associated with a prominent reduction in the number of late pre-B cells, but had little effect on proliferation of early pre-B cells. Inhibition of $p21^{ras}$ activity markedly reduced the life span of pre-B cells, due, at least in part, to downregulation of the expression of an antiapoptotic protein, Bcl-xL. Thus, the apparent role for $p21^{ras}$ activity in pre-B cell survival may explain the decreased numbers of late pre-B cells in Asn-17 *Ha-ras* TG. Consistent with this possibility, overexpression of Bcl-2 in Asn-17 *Ha-ras* TG reversed the reduction in the number of late pre-B cells undergoing immunoglobulin light chain gene (*IgL*) rearrangement and progressing to immature B cells. These results suggest that $p21^{ras}$ mediates effector pathways responsible for pre-B cell survival, which is essential for progression to the late pre-B and immature B stages.

Key words: B cell development • life span • immunoglobulin gene rearrangement • Bcl-xL • Bcl-2

Introduction

Committed B cell precursors undergo differentiation through several critical check points into surface immunoglobulin (sIg)[1] positive immature B cells (for a review, see reference 1). The earliest recognizable B cell precursors were identi-

H. Nagaoka and Y. Takahashi contributed equally to this work.

H. Nagaoka's current address is Laboratory of Molecular Immunology, The Rockefeller University, 1230 York Ave., New York, NY 10021.

Address correspondence to Toshitada Takemori, Department of Immunology, National Institute of Infectious Diseases, 1-23-1 Toyama, Shinjuku-Ku, Tokyo 162-8640, Japan. Phone: 81-3-5285-1156; Fax: 81-3-5285-1156; E-mail: ttoshi@nih.go.jp

[1]*Abbreviations used in this paper:* APC, allophycocyanin; BLNK, B cell linker protein; BM, bone marrow; BrdU, bromodeoxyuridine; EMA, ethidium monoazide; ERK, extracellular signal–regulated kinase; 3′ Eκ, 3′ Igκ enhancer; Eμ, *IgH* intronic enhancer; HSA, heat-stable antigen; LM, littermate controls; MAP, mitogen-activated protein; PI-3K, phosphatidylinositol 3-kinase; pre-BCR, pre-B cell antigen receptor; RT, reverse transcription; sIg, surface Ig; SL, surrogate L chain; TG, transgenic mice.

J. Exp. Med. © The Rockefeller University Press • 0022-1007/2000/07/171/11 $5.00
Volume 192, Number 2, July 17, 2000 171–181
http://www.jem.org/cgi/current/full/192/2/171

fied in bone marrow (BM) cells expressing CD43 and a low level of B220 (2, 3), and these cells progress to the pro-B stage. Successful IgH gene rearrangement and transient activation of surrogate light chain (SL) genes at the pro-B cell stage lead to expression of the pre-B cell antigen receptor (pre-BCR), which plays a pivotal role in allelic exclusion and in the pre-B transition (4–8). After expansion at the pre-B transition, pre-B cells increase the expression of the large isoform of Bcl-x (Bcl-xL; see references 9–11) and become competent to undergo rearrangement of the IgL gene, probably as a consequence of the late effect mediated by the pre-BCR (12–14).

The BCR and pre-BCR form a complex with the Igα and Igβ chains, which contain the immunoreceptor tyrosine-based activation motifs at the cytoplasmic region (15). Upon BCR stimulation, the tyrosine kinase Syk is recruited to the tyrosyl-phosphorylated immunoreceptor tyrosine-based activation motifs in Igα and Igβ cytoplasmic tails, followed by phosphorylation of a B cell linker protein BLNK, also known as SH2 domain–containing leukocyte protein of 65 kD (SLP-65), B cell adaptor containing SH2 domain (BASH), and BCA (for a review, see reference 16). Phosphorylated BLNK interacts with several signaling molecules, resulting in regulation of membrane-associated and soluble inositol polyphosphates and Ras–mitogen-activated protein (MAP) kinase cascades (16). The pre-BCR may mediate multiple effector pathways responsible for the pre-B transition, probably through Syk, BLNK, and phosphatidylinositol 3-kinase (PI-3K) (17–23); however, the regulatory mechanism of the pre-B transition by these molecules remains unclear.

Ras controls multiple signaling pathways by activation of PI-3K and the guanine nucleotide exchange factors for Ral, in addition to activation of Raf/MAP kinase kinases/extracellular signal–regulated kinase (ERK) (24). The activity of $p21^{ras}$ in early B cell development has been previously characterized by the expression of a dominant-inhibitory mutant of *Ha-ras* (Asn-17 *Ha-ras*; reference 25) in the earliest B cell precursors under the control of the proximal *lck* promoter and *IgH* intronic enhancer (Eμ) (26). High dose expression of Asn-17 *Ha-ras* caused a reduction in the number of the earliest recognizable B cell precursors and almost complete loss of pro-B and pre-B cells in the BM. This maturation arrest was partially rescued by expression of an activated form of Raf-1, suggesting a role for the Ras-Raf-1–mediated signaling cascade in the progression of differentiation from the earliest B cell precursors to the pro-B stage (26). In addition, expression of constitutively activated $p21^{ras}$ may result in developmental progression of the mutant pro-B cells in the absence of the H chain or recombination activating gene (RAG)-1, supporting the idea that $p21^{ras}$ could be involved in the signal cascade mediated by the pre-BCR (27, 28). However, the role for Ras in the progression of differentiation from the pro-B stage at physiological conditions remained to be elucidated.

In this study, we established transgenic mice (TG) that express Asn-17 *Ha-ras* under control of the *IgH* promoter, Eμ, and the 3′ Igκ enhancer (3′ Eκ). In agreement with the previous observation that the reporter gene linked to 3′ Eκ was transcriptionally activated at late-stage pro-B cell development (29), Asn-17 *Ha-ras* was fully expressed in B lineage cells after the early B cell precursor stage. Through the analysis of B cell development in the BM of TG, we demonstrated the novel finding that $p21^{ras}$ activity could be essential for pre-B cell survival, but not for proliferation of cells during the transition from the pro-B to early pre-B stages.

Materials and Methods

Establishment of Asn-17 Ha-ras TG. The plasmid containing Asn-17 *Ha-ras* was a gift of Dr. G.M. Cooper (Dana-Farber Cancer Institute, Boston, MA). The coding region of Asn-17 *Ha-ras* was amplified by PCR, and the 0.6-kb DNA fragment was subcloned in the expression vector containing the promoter of the V_H186.2 gene (30), Eμ (EcoRI–XbaI 0.8-kb fragments), 3′ Eκ (XbaI–SacI 0.8-kb fragments), SV40 intron (small t antigen), and polyA signals. The final construct was microinjected into pronuclei of C57BL/6 fertilized eggs. We bred transgene-positive founder mice with C57BL/6 mice, and established three independent transgenic lines, designated N-17-52, N-17-75, and N-17-95. These lines were maintained by breeding of heterozygous TG with nontransgenic littermates in sister–brother mating. To establish double TG, we crossed TG from N-17-95 with those from either N-17-52 or N-17-75. To determine the genotypes of offspring of littermates, we purified tail DNA and provided for Southern blot analysis by using HindIII as restriction enzyme and a 1.5-kb DNA fragment of SV40 polyA signal as a probe. In addition, the *bcl-2* transgene was introduced into the background of Asn-17 *Ha-ras* by crossing N-17-95 TG with Bcl-2 TG, which were purchased from The Jackson Laboratory.

FACS® Analysis. To analyze the early B cell precursors, BM cells were incubated with biotinylated anti-μ, anti-δ, anti-CD23 (BD PharMingen), antisyndecan (BD PharMingen), anti-NK1.1 (BD PharMingen), antierythroblasts (TER119), and anti–Gr-1 (BD PharMingen) mAbs. After washing, we stained cells with allophycocyanin (APC)-coupled B220 ($B220^{APC}$; BD PharMingen), FITC-conjugated anti-CD43 ($CD43^{FITC}$; BD PharMingen), and PE-coupled anti-CD24 (heat-stable antigen $[HSA]^{PE}$) mAbs (BD PharMingen). To analyze pro-B cells, we stained BM cells with $B220^{APC}$, $CD43^{FITC}$, PE-coupled anti–BP-1/6C3 ($BP\text{-}1^{PE}$; BD PharMingen), and biotinylated anti-CD24 mAbs. To analyze pre-B cells, we incubated BM cells with biotinylated mAbs (anti-μ, anti-δ, anti-CD23, anti-NK1.1, antierythroblasts, and anti–Gr-1), followed by staining with anti-$B220^{APC}$, anti-$CD43^{FITC}$, and anti–$BP\text{-}1^{PE}$ mAbs. After washing, cells were incubated with Texas red–coupled UltraAvidin ($avidin^{TEX}$; Leinco Technologies, Inc.). To analyze immature and circulating B cells in the BM, we stained cells with anti-$B220^{APC}$, anti-HSA^{PE}, biotinylated anti-CD23, FITC-coupled anti-μ (anti-μ^{FITC}), and anti-δ^{FITC} mAbs, followed by incubation with $avidin^{TEX}$. Cells were resuspended in staining buffer containing propidium iodide (5 μg/ml) and analyzed with a FACS Vantage™ (Becton Dickinson) equipped with appropriate filters for five-color analysis in a dual argon laser (488 nm)/dye laser (599 nm) system (30).

Analysis of pre-BCR Expression. BM cells were stained with ethidium monoazide (EMA; Molecular Probes) and a mixture of anti-μ^{FITC}, anti-δ^{FITC}, anti-$CD23^{FITC}$, anti-$B220^{TEX}$, and $BP\text{-}1^{PE}$ mAbs. After washing, the cells were left for 20 min under UV light for irreversible photolytic coupling of EMA to the cellular DNA. Thereafter, the cells were washed with PBS and fixed with

2% formaldehyde for 30 min at room temperature. The cells were then washed and permeabilized with a solution of 0.5% saponin in PBS containing 1% BSA, 0.25 mM EDTA, and 10 mM Hepes, together with 100 μg/ml of 2.4G2 and MOPC21, followed by staining in combination with biotinylated mAb SL156 (31) at the first step, and streptavidin-coupled APC at the second step.

Cell Cycle Analysis. BM cells were stained with EMA and with $B220^{FITC}$ and anti-HSA^{PE} mAbs. After washing, the cells were left under UV light, washed, and fixed with 2% formaldehyde. The cells were then extensively washed and permeabilized with 0.5% saponin, followed by incubation for 30 min with Hoechst 33342 (1 μg/ml; Sigma-Aldrich) at room temperature. DNA contents were analyzed with a FACS Vantage™ equipped with the appropriate filters for four-color analysis in a dual argon laser (488 nm)/UV laser (351/360 nm) system. Excitation of the Hoechst 33342 was carried out by UV light with a maximum wavelength of 351/360 nm, and fluorescence of the Hoechst 33342 was achieved by UV transmission at 424 ± 22 nm.

Purification of BM B Cells. To enrich B cells, we incubated BM cells with biotinylated mAbs (anti–Gr-1, anti–Mac-1, anti-NK1.1, and anti-CD90). After washing, cells were incubated with streptavidin-coated microbeads and separated on a MACS column (Miltenyi Biotec). To purify pre-B cells and recirculating B cells, we stained enriched B cells with anti-$B220^{APC}$, anti-HSA^{PE}, anti-μ^{FITC}, anti-δ^{FITC}, and anti-$CD23^{FITC}$ mAbs. To purify early B cell precursors, we stained enriched B cells with anti-$B220^{APC}$, anti-$CD43^{FITC}$, and anti-HSA^{PE} mAbs and with a mixture of biotinylated mAbs (antisyndecan, anti-μ, anti-δ, and anti-CD23). To purify pro-B cells, we stained BM cells with anti-$B220^{APC}$, anti-$CD43^{FITC}$, biotinylated anti-HSA, and anti–BP-1^{PE} mAbs. After washing, cells were incubated with $avidin^{TEX}$. Viable cells were sorted under the forward and side scatter lymphocyte gate on a FACS Vantage™. Reanalysis of sorted pre-B cells showed a purity between 89 and 94%.

Analysis of Pre-B Cell Proliferation. To detect the uptake of 5-bromo-2′-deoxyuridine (BrdU) by BM B cells, mice were injected intraperitoneally with a single dose of 1 mg BrdU (Sigma-Aldrich). After injection, pre-B cells were purified from individual animals by FACS® sorting and provided for staining with or without FITC-conjugated anti-BrdU mAb (Becton Dickinson), as described previously (30), or with or without mouse anti-BrdU mAb (Oncogene Research Products), followed by staining with affinity-purified goat anti–mouse IgG Fc fragments that were conjugated with FITC (American Qualex). After washing, cells were incubated with anti-$B220^{APC}$ mAb and propidium iodide. For staining controls, the same staining procedure was undertaken for pre-B cells that were purified from C57BL/6 mice and a B cell lymphoma, WEHI231, that was labeled in vitro with or without BrdU. The samples were examined by confocal laser microscopy (LSM410 Laser Scan microscope; Carl Zeiss, Inc.).

Cell Culture. We enriched B cells from pooled spleens of TG and littermate controls (LM) from N-17-95 using a MACS system. 5×10^6 enriched B cells (>90% $B220^+$) were cultured in the presence or absence of affinity-purified $F(ab')_2$ goat anti-μ antibody (Jackson ImmunoResearch Laboratories) or anti-CD40 mAb (BD PharMingen), as described previously (11). After several time points, cells were harvested and subjected to Western blot analysis for detection of Bcl-xL.

Western Blot Analysis. Cells were lysed in RIPA buffer for analysis of $p21^{ras}$, or in a buffer containing 1% NP-40, 137 mM NaCl, 1 mM $MgCl_2$, 0.1 mM $CaCl_2$, 20 mM Tris-HCl (pH 9.0), 10% glycerol, 0.3 mg papain, 30 μg/ml pancreas extract, 2 μg/ml chymotrypsin, 0.5 μg/ml thermolysin, 20 μg/ml trypsin for analysis of Bcl-xL. The same amount of protein in each sample was separated by SDS-PAGE on a 12 or 15% gel and transferred to a polyvinylidene (PVDF) membrane (Millipore). Blots were incubated with rat anti-Ras mAb (Y13-259; a gift from Dr. Nakafuku, Nara Institute of Science and Technology, Ikoma, Japan), mouse anti-Ras mAb (Ab-3; Oncogene Research Products), or mouse anti–Bcl-x mAb (Transduction Laboratories). After washing, blots were incubated with anti–rat Ig or anti–mouse Ig antibody coupled with peroxidase (Amersham Pharmacia Biotech). After washing, $p21^{ras}$ or Bcl-xL was visualized by the ECL system (Amersham Pharmacia Biotech) as described previously (32). In addition, the blot was probed with mouse anti–β-tubulin mAb (Sigma-Aldrich).

In Vitro MAP Kinase Assay. Resting B cells were purified from pooled spleens of Asn-17 *Ha-ras* TG and age-matched wild-type C57BL/6 mice and stimulated with $F(ab')_2$ goat anti–mouse IgM polyclonal antibody (Jackson ImmunoResearch Laboratories). These cells were provided for an in vitro kinase assay for endogenous ERK activity, as described previously (32).

Semiquantitation of mRNA by Reverse Transcription PCR. Messenger RNA of sorted cells was purified, and first-strand cDNA was synthesized. Aliquots of cDNA were serially diluted fivefold and provided for reverse transcription (RT)-PCR by using a Premix Taq (Takara Shuzo Co., Ltd.) or Super Taq Premix (Sawady Technology). As a control, β-actin cDNA was amplified by primers CCTAAGGCCAACCGTGAAAAG and TCTTCATGGTGCTAGGAGCCA. *H-ras* cDNA was amplified by a set of primers, TGACCATCCAGCTGATCCAG and TTGCAGCTCATGCAGCC. In some experiments, additional amplification was performed by using nested primers TGCCATCAACAACACCAAG and GCAGCCAGGTCACACTGGT. The reaction conditions used for each primer set were as follows: β-actin, 94°C for 1 min, 58°C for 1 min, and 72°C for 1.5 min, 40 cycles; H-*ras* and H-*ras* nested, 94°C for 1 min, 60°C for 1 min, 72°C 1.5 min, 45 cycles and 25 cycles, respectively.

Semiquantitation of Rearranged Igκ Gene by PCR. High molecular mass genomic DNA was extracted by the proteinase K method from purified pre-B cells. The PCR cycle was repeated 26–32 times. PCR reactions were performed to detect rearrangements of *Igκ* as described previously (33). PCR products were detected by Southern blot hybridization to specific radiolabeled Jκ probe (1.7-kb SphI–PstI fragment) or ethidium bromide staining. To detect *bcl-6*, we used the following set of primers: mBCL-6EX5, 5′-GGCTCAATAATCTCGTGAAC-3′, and mBCL-6EX6, 5′-AGTGACTCTCACTGCTGCTT-3′.

Results and Discussion

Establishment of TG Expressing Asn-17 Ha-ras Transgene in B Cells. We constructed the transgene by insertion of the dominant-inhibitory mutant of Asn-17 *Ha-ras* (25) in an expression cassette consisting of the V_H gene promoter (Vp), Eμ, and 3′ Eκ (Fig. 1 A). The transgene was injected into fertilized eggs of C57BL/6 mouse origin, and three independent transgenic lines, designated N-17-52, N-17-75, and N-17-95, were analyzed. As shown in Fig. 1 B, RT-PCR analysis showed the greater expression of *ras* transcripts in pre-B (top) and pro-B cells (middle) in TG from line N-17-95 than LM. In contrast, this transcript was undetectable in early B cell precursors (bottom, a) without additional amplification by nested PCR (bottom, c). These

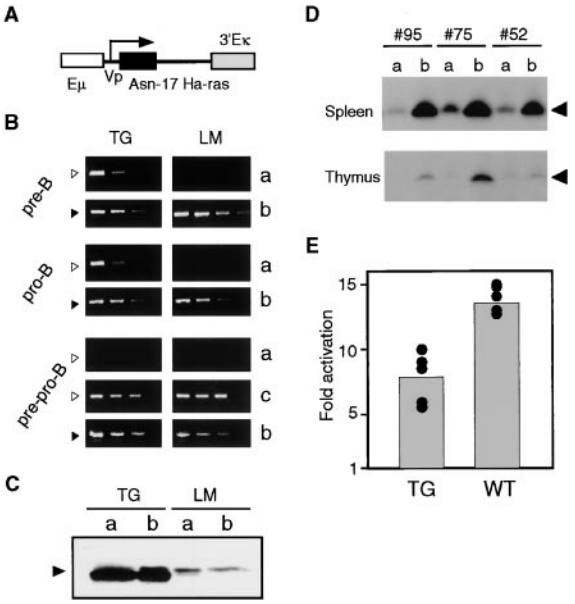

Figure 1. (A) Schematic representation of Asn-17 *Ha-ras* transgene. Asn-17 *Ha-ras* cDNA (black box) was inserted into the vector containing V_H186.2 gene promoter (Vp), an Eμ fragment (white box), and a 3′ Eκ fragment (gray box). (B) Expression of *ras* in BM B cells of TG and LM of N-17-95. Aliquots of cDNA, synthesized from mRNA of purified early B cell precursors (bottom), pro-B cells (middle), and pre-B cells (top), were serially diluted fivefold, and Ras transcripts (white arrowheads in a) were analyzed by RT-PCR assays with β-actin used as internal control (black arrowheads in b), or by additional amplification using *Ras* nested primer (white arrowhead in c). The first dilution of all samples is 1:5. (C) Expression of $p21^{ras}$ protein in purified pre-B cells (a) and recirculating B cells (b) in the BM of TG and LM of N-17-95. Shown is a representative immunoblot performed with 10 μg total cellular protein. $p21^{ras}$ was visualized with the ECL system (arrowhead). (D) Expression of $p21^{ras}$ protein in splenocytes of TG (b) and LM (a) from N-17-95 (#95), N-17-75 (#75), or N-17-52 (#52). Shown is a representative immunoblot performed with 100 μg total cellular protein of splenocytes (top) and thymocytes (bottom). $p21^{ras}$ was visualized with the ECL system (arrowheads). (E) Resting B cells of TG from N-17-95 and age-matched C57BL/6 mice (WT) were stimulated with anti-IgM antibody (50 μg/ml) for 2 min. The same amount of each extract was incubated with anti-ERK2 antibody, and the immunoprecipitates were subjected to an in vitro kinase assay with myelin basic protein (MBP) as a substrate. Relative radioactivities of phosphorylated MBP from each immunoprecipitate were quantitated with an Image Analyzer (Fuji Photo Film Co., Ltd.). The extent of activation was calculated by comparison between the radioactivity given by the immunoprecipitates of stimulated cells and that of unstimulated cells. Bars represent the average values of fold activation of ERK in TG and LM, summarized from five independent experiments (filled circles).

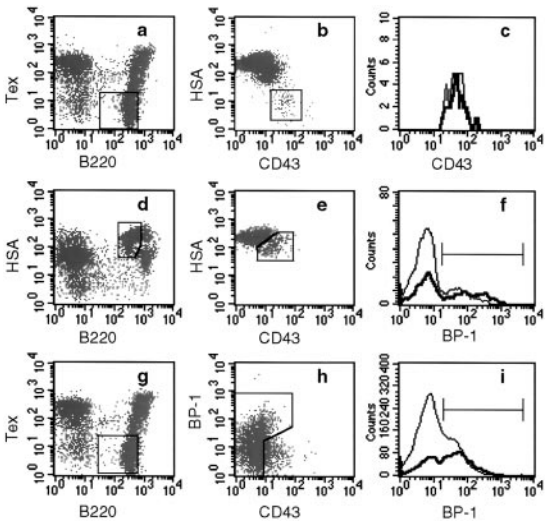

Figure 2. Flow-cytometric analysis of B cell development in the BM of Asn-17 *Ha-ras* TG and LM from N-17-95. Dead cells were detected by uptake of propidium iodide and excluded from analysis by gating. Viable cells were analyzed under a lymphocyte gate on forward by side light scatter. BM cells stained with biotinylated mAbs (anti-μ, anti-δ, NK1.1, anti–Gr-1, anti–Mac-1, antisyndecan, and TER119) in combination with $avidin^{TEX}$ (Tex) were gated out in $B220^{dull/+}$ cells (a), and $CD43^{+}HSA^{dull}$ cells were analyzed (b). A histogram in c represents the relative number of early B cell precursors in TG (bold line) and LM (thin line). To analyze pro-B cells, $HSA^{+}CD43^{+/dull}$ cells (e) were gated in a $B220^{dull/+}HSA^{high/+}$ population (d) and $BP\text{-}1^{-}$ cells were monitored as pro-B cells (f). A histogram in f represents the relative number of pro-B cells in TG (bold line) and LM (thin line). To analyze pre-B cells, BM cells stained with biotinylated mAbs (anti-μ, anti-δ, anti-CD23, NK1.1, anti–Gr-1, TER119, and anti-CD90)/$avidin^{TEX}$ (Tex) were gated out in B cells (g). Subsequently, expression of CD43 and BP-1 was analyzed (h), and the number of $CD43^{dull/-}BP\text{-}1^{+}$ and $CD43^{-}BP\text{-}1^{-}$ cells was estimated as $BP\text{-}1^{+}$ and $BP\text{-}1^{-}$ pre-B cells, respectively, in TG (bold line) and LM (thin line) (i). The horizontal bar in the histogram represents the region with $BP\text{-}1^{+}$ cells.

results suggested that the transgene could be fully activated in BM B cells after the early B cell precursor stage.

Immunoblot analysis showed a remarkable expression of $p21^{ras}$ in pre-B and circulating B cells in the BM of N-17-95 TG, ~10-fold above the level of LM (Fig. 1 C). Fig. 1 D shows the expression of $p21^{ras}$ in splenocytes in N-17-75 and N-17-95 TG, approximately fivefold above the level of LM, and, to a lesser extent, in N-17-52 TG (top). The level of $p21^{ras}$ expression was low in the thymus of TG and LM, except for TG from N-17-75 (bottom). These results suggest that transgenic B cells expressed $p21^{Asn\text{-}17\ Ha\text{-}ras}$ exceeding the level of endogenous $p21^{ras}$.

Fig. 1 E shows that ERK activation by IgM stimulation was reduced in resting B cells of TG from line N-17-95 by 30–50% of the wild-type C57BL/6 B cells. Similar results were obtained by analysis of resting B cells of TG N-17-52 and N-17-75 (data not shown), suggesting that expression of $p21^{Asn\text{-}17\ Ha\text{-}ras}$ may significantly inhibit endogenous $p21^{ras}$ activity in B cells.

Expression of Asn-17 Ha-ras Transgene Preferentially Reduced the Number of Pro-B Cells and Late Pre-B Cells in the BM. As shown in Fig. 2, we evaluated B cell development in the BM of Asn-17 *Ha-ras* TG by five-color flow cytometry (30), according to the strategy established by Hardy and colleagues (2, 3). To analyze early B cell precursors ($B220^{dull}CD43^{+}HSA^{dull}$), we excluded non-B lineage cells, Ig^{+} cells, and plasma cells in $B220^{dull/+}$ cells (Fig. 2 a), and monitored $CD43^{+}HSA^{dull}$ cells (Fig. 2 b). To analyze pro-B cells ($B220^{dull}CD43^{dull}HSA^{+}$), we gated $B220^{dull}HSA^{+/high}$ BM cells that consisted of pro-B cells, pre-B cells, and immature B cells (Fig. 2 d). Subsequently, $CD43^{+/dull}HSA^{+}$ cells were gated in a $B220^{dull}HSA^{+/high}$ population (Fig. 2 e), and $BP\text{-}1^{-}$ pro-B cells were analyzed (Fig. 2 f). To analyze pre-B cells ($B220^{dull}CD43^{dull/-}$

HSA^{high}), we excluded immature and mature B cells and non-B lineage cells (Fig. 2 g) and monitored B220^{dull}CD43$^{dull/-}$ cells (Fig. 2 h), which can be divided into BP-1$^-$ and BP-1$^+$ fractions (Fig. 2 i).

TG at ages between 10 and 15 wk from N-17-95 (Fig. 2 and Fig. 3 A), N-17-75 (Fig. 3 B), and N-17-52 (Fig. 3 C) displayed a reduction in the number of pro-B cells by 40–50% of LM. The number of early B cell precursors was comparable between TG and LM, consistent with the results illustrated in Fig. 1 B. Among pre-B cell subsets, TG from N-17-95 and N-17-75 reduced the number of BP-1$^-$ cells, four- to fivefold below the level of LM, more prominently than the reduction in the number of BP-1$^+$ cells (Fig. 3, A and B). A similar phenotype was observed in N-17-52 TG, although the reduction in pre-B cells was less marked (Fig. 3 C). Preferential reduction in the number of pro-B and BP-1$^-$ pre-B cells was also observed in young N-17-95 TG (Fig. 3 D). RT-PCR analysis suggested that transgenic BP-1$^+$ and BP-1$^-$ pre-B cells expressed Asn-17 *Ha-ras* transcripts at comparable levels (data not shown), excluding the possibility that preferential reduction in the number of BP-1$^-$ pre-B cells was due to high levels of transgene expression in this subset.

We crossed N-17-95 TG with either N-17-52 or N-17-75 and analyzed B cell development in the BM of the offspring of the littermates (Fig. 4). The reduction in the number of B cells was dose sensitive, except for the early B cell precursors (pre–pro-B) that almost sustained the number at comparable levels in single and double TG as well as LM. The dose effect was more pronounced in N-17-95/N-17-75 double TG (Fig. 4 B) than in N-17-95/N-17-52 double TG (Fig. 4 A). Although the number of BP-1$^+$ pre-B cells was reduced in N-17-95/N-17-75 double TG, by 3-fold below that of LM, the reduction in the number of pro-B and BP-1$^-$ pre-B cells was more prominent, 15- and 30-fold below the level in LM, respectively (Fig. 4 B). Thus, a preferential reduction in the number of BP-1$^-$ cells

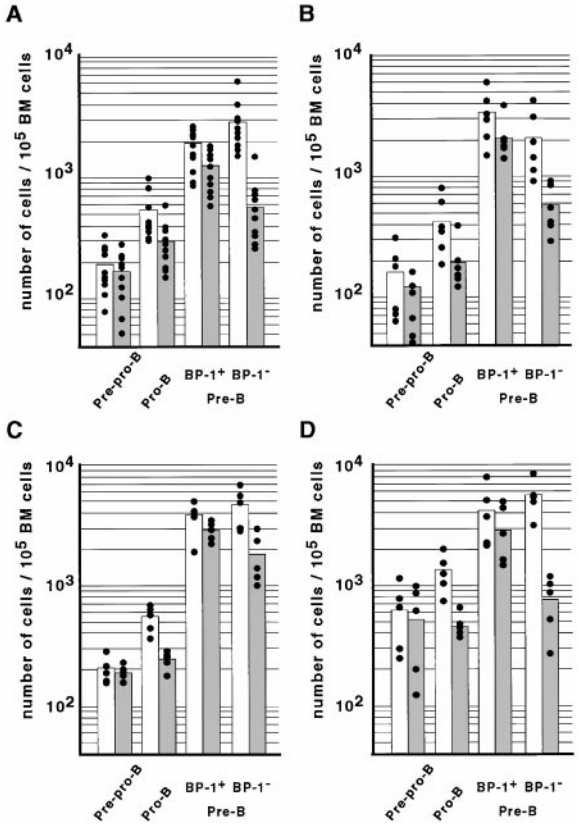

Figure 3. Preferential reduction in the number of pro-B and BP-1$^-$ pre-B cells in the BM of Asn-17 *Ha-ras* TG. BM cells were prepared from individual TG and LM from N-17-95 (A), N-17-75 (B), or N-17-52 (C) of 10–15 wk of age and N-17-95 at 5–6 wk of age (D). The number of early B cell precursors (Pre-pro-B), pro-B, and BP-1$^+$ and BP-1$^-$ pre-B cells was estimated by FACS®, and the number per 10^5 viable BM cells was recalculated (y-axis). The results show the average number of cells in TG (gray bars) and LM (white bars), summarized from five to eight independent experiments. Circles represent the results for individual animals.

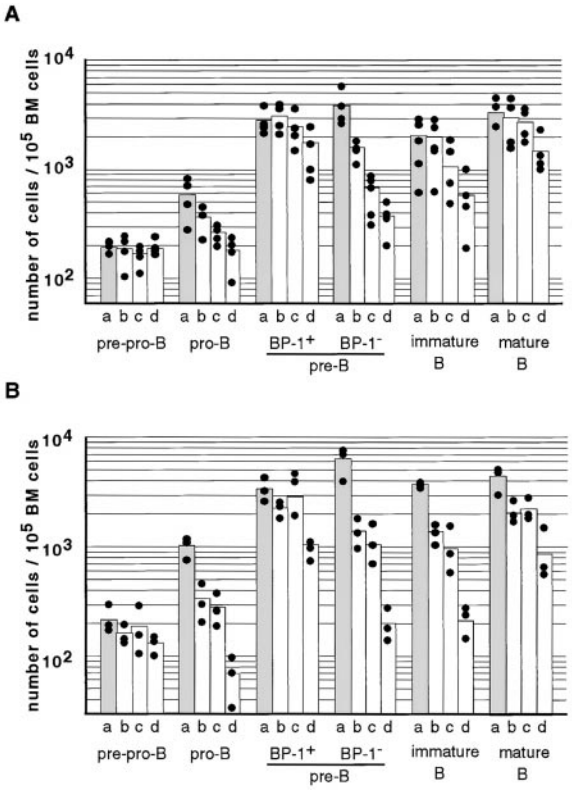

Figure 4. Preferential reduction in the number of pro-B and late pre-B cells by expression of Asn-17 *Ha-ras* transgene at different gene dosages. A set of offspring with the genotype of N-17-52 (b), N-17-95 (c), N-17-52/N-17-95 (d), and nontransgenic control (a) in A, or those with the genotype of N-17-75 (b), N-17-95 (c), N-17-75/N-17-95 (d) and nontransgenic control (a) in B were obtained by crosses between N-17-95 and N-17-52 (A) or N-17-95 and N-17-75 (B), respectively. BM cells were prepared from individual animals at 12–13 wk of age and subjected to FACS® analysis. Bars represent the average number of early B cell precursors (pre-pro-B), pro-B cells (pro-B), and BP-1$^+$ and BP-1$^-$ pre-B cells (pre-B), immature B cells (immature B), and recirculating B cells (mature B) in the BM of TG (white bars) and LM (gray bars). Filled circles represent the number of cells in individual animals. The results were summarized from three independent experiments using animals of the same age.

in pre-B cell subsets was a common feature in animals that expressed the Asn-17 *Ha-ras* transgene at different doses.

BP-1 is expressed at the pro-B to pre-B transition, whereas the expression is downregulated at the pre-B to immature B transition (2, 34). We observed that 30–50% of BP-1^+ pre-B cells were labeled with BrdU by a single injection of the reagent, three- to fourfold above the level of BP-1^- pre-B cells (data not shown). Assuming that BP-1^+ and BP-1^- cells could be enriched by early and late pre-B cells, respectively, we investigated whether pre-B cells were more susceptible at the late stage than at the early stage to any effect caused by inhibition of $p21^{ras}$ activity. As shown in Fig. 5 A, we analyzed the expression of pre-BCR in $Ig^-CD23^-B220^{dull}$ B cells of N-17-95 TG, N-17-95/N-17-52 double TG, and nontransgenic LM by using mAb SL156 (31), which recognizes a conformational epitope on the μ and SL chain complexes. $Ig^-CD23^-B220^{dull}$ B cells contained pre-B cells and small numbers of pro-B and the earliest B cell precursor cells (data not shown).

As shown in Fig. 5 B, pre-BCR^+ cells were detected in the BP-1^+ and BP-1^- subsets of the $B220^{dull}Ig^-CD23^-$ B cells. Because the pre-BCR is transiently expressed at the late pro-B to early pre-B transition (35), we speculated that pre-BCR^+BP-1^- cells would be at the late pro-B stage, in the process of maturation to BP-1^+ pre-B cells. The number of pre-BCR^-BP-1^- cells was prominently reduced by the expression of Asn-17 *Ha-ras* transgene in a dose-dependent manner, whereas a reduction in the number of pre-BCR^+ and pre-BCR^- BP-1^+ cells was less marked. Because pre-BCR^+ pre-B cells enter the S phase of cell cycle at a high frequency (35), these results support the notion that inhibition of $p21^{ras}$ activity does not have much effect on proliferating cells at the late pro-B to the early pre-B transition.

The BP-1^+ cells consisted of a minor population in immature B cells at comparable levels between LM and TG from N-17-95 or N-17-95/N-17-52 (data not shown), excluding the possibility that inhibition of $p21^{ras}$ caused an abnormality in the expression of BP-1. In addition, we did not detect any B cells with an aberrant phenotype in either the BM or spleen of the TG within the limitations of the FACS® analysis.

Inhibition of $p21^{ras}$ Activity Caused a Short Life Span of Pre-B Cells. B cells proliferate efficiently at the transition from pre-BCR^+ pre-B to large pre-B cells (35), resulting in a substantial expansion of cell population size (35, 36). To investigate the role of $p21^{ras}$ in pre-B cell proliferation, we analyzed the DNA content of $B220^{dull}HSA^{+/high}$ B cells in the BM of N-17-95 TG, N-17-95/N-17-52 double TG, and LM using flow cytometry (Fig. 6, A and B). As summarized in Fig. 6 C, 13–30% of $B220^{dull}HSA^{+/high}$ B cells entered the S phase of cell cycle in the BM of LM, at a comparable level to that of pre-B cells (35). Although $B220^{dull}HSA^{+/high}$ B cells in TG and LM were composed of pre-B cells, immature B cells, and pro-B cells (83–86, 12–15, and 1.3–3%, respectively), proliferating $B220^{dull}HSA^{+/high}$ cells could comprise largely pre-B cells, because immature B cells are mostly at a resting state in TG and LM (36; data not shown). As shown in Fig. 6 C, the number of proliferating cells was reduced in N-17-95 TG, by 60% of LM, whereas the reduction in the number of resting $B220^{dull}HSA^{+/high}$ cells was more significant, threefold below the level found in LM. As shown in Fig. 6, D and E, the number of resting $B220^{dull}HSA^{+/high}$ cells was remarkably reduced in N-17-95/N-17-52 double TG, seven- to eightfold below the level in LM. In contrast, the number of cycling $B220^{dull}$ $HSA^{+/high}$ cells was almost comparable between N-17-95 TG and N-17-95/N-17-52 double TG. These results raised the possibility that the late pre-B transition, but not the early pre-B transition, could be highly susceptible to an effect caused by the inhibition of $p21^{ras}$ activity.

As shown in Fig. 6 F, to investigate further the role of $p21^{ras}$ in the proliferation and accumulation of pre-B cells, we injected a single dose of BrdU into TG and LM from N-17-95. Pre-B cells were purified from the BM of individual animals at 2, 40, and 62 h after injection and stained with anti-BrdU mAb, followed by examination under confocal microscopy (30). In agreement with the results depicted in Fig. 6, B and D, the number of pre-B cells incorporating BrdU 2 h after injection was comparable between

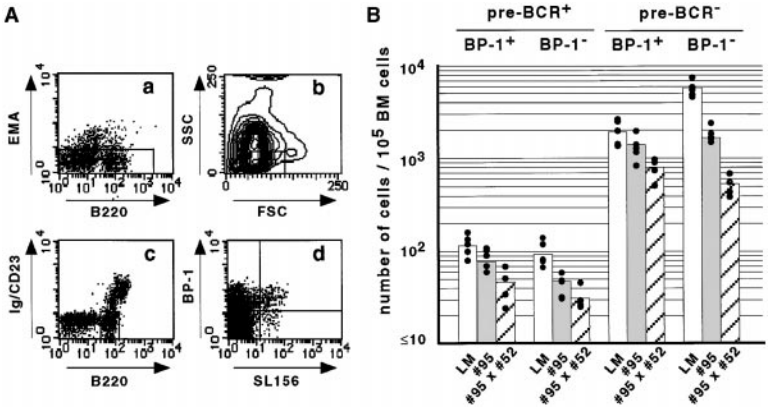

Figure 5. Inhibition of $p21^{ras}$ activity caused a preferential reduction in the number of pre-$BCR^-BP\text{-}1^-$ pre-B cells. BM cells were prepared from a set of offspring with the genotype of N-17-95 (#95), N-17-95/N-17-52 (#95 × #52), and nontransgenic controls (LM). These cells were stained with EMA and with anti-$B220^{TEX}$, anti–BP-1^{PE}, anti-IgM^{FITC}, anti-IgD^{FITC}, and anti-$CD23^{FITC}$ mAbs. After washing, the cells were fixed with formaldehyde, permeabilized with saponin, and stained with biotinylated mAb SL156, followed by staining with APC-coupled streptavidin at the second step. The cells were then analyzed under a lymphocyte gate on forward by side light scatter (A, b) after exclusion of EMA^+ cells from analysis by gating (A, a). $B220^+Ig^+CD23^+$ cells were gated out (A, c) and $B220^{dull}$ cells stained with or without BP-1 were analyzed for the expression of SL156 (A, d). In B, the results show the average number of $SL156^+$ (pre-BCR^+) cells in BP-1^+ or BP-1^- pre-B cells in the mice with the genotype of #95 × # 52 (striped bars), #95 (gray bars), and LM (white bars), summarized from two independent experiments. Circles represent the data from individual animals.

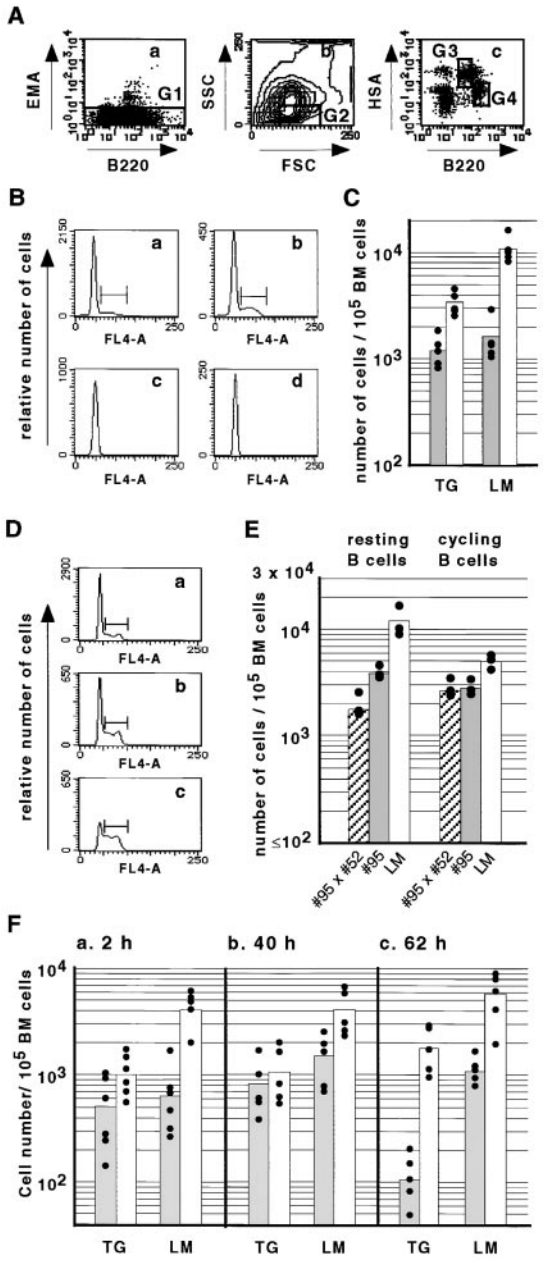

Figure 6. Inhibition of p21*ras* activity reduced the life span of pre-B cells. In A, BM cells were stained with anti-B220^{FITC} and anti-HSA^{PE} mAbs and with EMA. After fixation and permeabilization with saponin, cells were stained with Hoechst 33344, followed by FACS® analysis for B220^{dull}HSA$^{+/high}$ B cells (c, G3) and B220^{+}HSA^{dull} circulating B cells (c, G4), as a control, under a lymphocyte gate on forward (FSC) by side (SSC) light scatter (A, b, G2) after exclusion of EMA^{+} cells from analysis (A, a, G1). In B, DNA content of pre-B (B220^{dull}HSA$^{+/high}$) cells of TG from N-17-95 (b) and LM (a) and that of B220^{+}HSA^{dull} circulating B cells in the BM of TG (d) and LM (c) is shown in each histogram. The average number of cells at a resting state (white bars) and in the S phase of the cell cycle (gray bars) was calculated from the results in B and plotted in C. Circles represent the data from individual animals at 12–14 wk of age. In D, DNA content of pre-B cells of TG with the genotype of N-17-95 (#95, b), N-17-95/N-17-52 (#95 × #52, c), and LM (a) is shown in each histogram. The average number of resting and cycling pre-B cells in LM (white bars), #95 (gray bars), and #95 × #52 (striped bars) was calculated from the results in D and plotted in E. Circles represent the data from individual animals at 6–7 wk of age. (F) Pre-B cells were purified from the BM of N-17-95 TG (TG) and nontransgenic LM (LM) after injection of BrdU (1 mg). Cells were mounted on a glass slide, fixed, and stained with anti-BrdU mAb. Frequency of labeled cells was determined under confocal microscopy, and the number of labeled (gray bars) and nonlabeled cells (white bars) was calculated based on the total number of viable pre-B cells in BM cells for sorting. Bars represent the average number of cells. Filled circles represent the results for individual animals at 12–15 wk of age.

TG and LM, whereas in TG the number of nonlabeled pre-B cells was reduced approximately fourfold below that of LM (Fig. 6 F, a). BrdU-labeled pre-B cells increased in number in the BM of LM 40 h after injection (Fig. 6 F, b), indicating accumulation of pre-B cells after several successive proliferations at the transition from late pro-B to early pre-B cells (35, 36). The number of labeled cells in TG was half that in LM 40 h after injection (Fig. 6 F, b), followed by a remarkable reduction in number 62 h after injection, ~10-fold below the level of LM (Fig. 6 F, c), suggesting that inhibition of p21*ras* activity may affect the life span of pre-B cells. The number of labeled cells in the immature B cells was significantly low in TG relative to LM 40 and 62 h after injection (data not shown), excluding the possibility that transgenic pre-B cells progress to the stage of immature B cells within periods shorter than required for the cells in the LM.

Expression of Bcl-xL Was Downregulated in Transgenic Pre-B Cells. Bcl-xL plays a critical role in regulating pre-B cell survival (9–11). To investigate whether the short life span of transgenic pre-B cells might reflect the low levels of Bcl-xL expression, we analyzed the expression by Western blotting analysis in pre-B cells that were purified from the pooled BM of TG and LM of N-17-95. Fig. 7 A shows that pre-B cells expressed Bcl-xL, as previously reported (11), and the level of expression was reduced in transgenic pre-B cells, two- to threefold below the level in LM. RT-PCR analysis showed that BP-1^{+} and BP-1^{-} pre-B cells expressed *bcl-xL* transcripts at comparable levels in both N-17-95 TG and LM, but the level of expression was significantly low in TG relative to LM (data not shown). These results support the notion that p21*ras* activity is associated with pre-B cell survival, at least in part through regulation of Bcl-xL expression.

Bcl-xL expression reaches its maximum at the small pre-B stage (10). Although the mechanism responsible for upregulation of Bcl-xL at the pre-B stage remains unknown, pre-BCR–mediated signaling would be one of the candidate elements. Considering that the pre-BCR and BCR may activate several common signaling molecules (37), including Ras (27, 28), we set out to determine to what extent the expression of p21$^{Asn\text{-}17}$ *Ha-ras* has an inhibitory effect in the upregulation of Bcl-xL in transgenic B cells via BCR stimulation. As reported previously (11), the expression of Bcl-xL proteins was upregulated in B cells upon IgM stimulation (Fig. 7 B); however, the level was reduced in transgenic B cells to approximately two- to threefold below that of LM. In addition, the expression of Bcl-xL mediated by

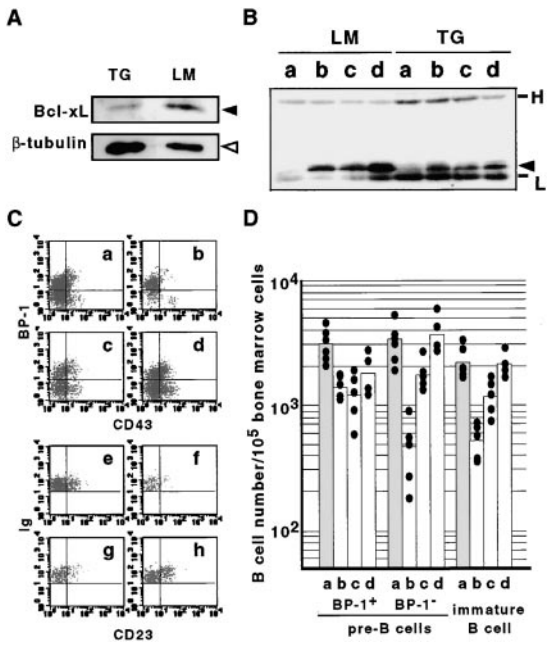

Figure 7. (A) Expression of Bcl-xL protein in pre-B cells. Pre-B cells were purified from the pooled BM cells of TG and LM from N-17-95. The cell lysate at 10 μg total protein was separated by SDS-PAGE on a 12% gel, transferred to a PVDF membrane, and visualized by anti–Bcl-x antibody in the ECL system (top). The same blot was probed with anti–β-tubulin mAb (bottom). Shown is a representative result from three independent experiments. (B) Expression of Bcl-xL protein in splenic B cells upon IgM and CD40 stimulation. B cells of TG and LM from N-17-95 were cultured in the absence (a) or presence of anti-IgM antibody (60 μg/ml in b; 20 μg/ml in c), or anti-CD40 mAb (3 μg/ml, d). After 10 h of cultivation, cell lysates were provided for Western blot analysis for detection of Bcl-xL (arrowhead). H and L represent the IgH and IgL chains of cultured B cells, respectively. Shown is a representative result from three independent experiments. (C) Coexpression of Bcl-2 restored the number of BP-1$^-$ pre-B and immature B cells in N-17-95 TG. BM cells were prepared from individual offspring with the genotype of N-17-95/Bcl-2 double TG (c and g), N-17-95 TG (b and f), Bcl-2 TG (d and h), and nontransgenic control (a and e). Shown is a representative result of dot blot analysis for BP-1$^+$ and BP-1$^-$ pre-B cells (a–d) and immature B cells (e–h). (D) The number of BP-1$^+$ and BP-1$^-$ pre-B and immature B cells in LM (a), N-17-95 TG (b), N-17-95/Bcl-2 double TG (c), and Bcl-2 TG (d). Bars represent the average number of cells, summarized from four independent experiments using animals at the same age between 12 and 15 wk. Circles represent the number of cells in individual animals.

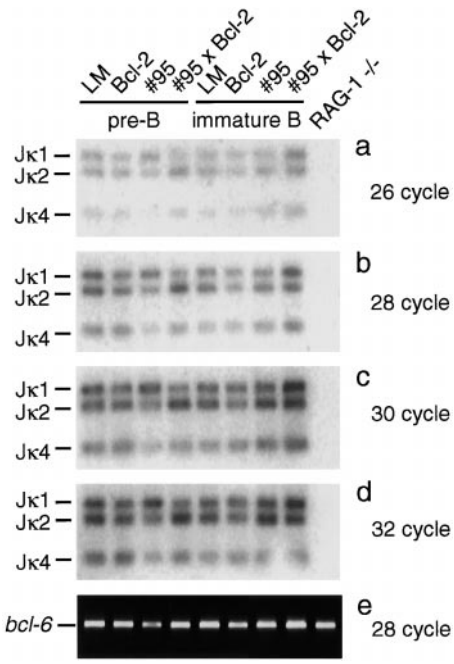

Figure 8. Relative frequency of V_κ to J_κ recombination in pre-B cells of TG expressing Asn-17 *Ha-ras* and *bcl-2* transgenes. Genomic DNA was prepared from pre-B cells (pre-B) and immature B cells (immature B) that were purified from the pooled BM of N-17-95 TG (#95), Bcl-2 TG (Bcl-2), N-17-95/Bcl-2 double TG (#95 × Bcl-2), and nontransgenic LM (LM). Endogenous V_κ–J_κ regions were amplified by PCR with 26 (a), 28 (b), 30 (c), and 32 (d) cycles. DNA was separated by agarose gel electrophoresis, and rearrangements were detected by Southern hybridization with the J_κ region DNA as a probe. Similar results were obtained in three independent experiments. For normalization of the results, *bcl-6* was amplified by PCR with 28 cycles (e).

CD40 was reduced by the expression of p21$^{\text{Asn-17 } Ha\text{-}ras}$ (Fig. 7 B, d). These results suggest that p21^{ras} may play a role in Bcl-xL expression in B cells mediated by extracellular stimuli, which might occur at the pre-B stage.

Coexpression of Bcl-2 Restored the Number of Late Pre-B Cells in Asn-17 Ha-ras TG. The results illustrated in Figs. 6 and 7 A are compatible with the view that reduction in the number of late pre-B cells in Asn-17 *Ha-ras* TG may reflect an abnormality in pre-B cell survival. Because Bcl-2 and Bcl-xL may inhibit cell death through a common pathway (for a review, see reference 38), we examined whether introduction of *bcl-2* into the background of Asn-17 *Ha-ras* transgene might rescue the reduction in the number of pro-B and BP-1$^-$ pre-B cells (Fig. 6, C and D).

We observed that the number of early B cell precursors was indistinguishable between offspring of crosses between N-17-95 and Bcl-2 TG (data not shown). We could draw no definite conclusion on the effect of Bcl-2 in the number of pro-B cells in Asn-17 *Ha-ras* TG. Bcl-2 TG and Bcl-2/N-17-95 double TG prominently expanded Ig$^+$ B cells with the phenotype HSA$^+$B220^{dull}CD43^{dull} in the BM (data not shown), which caused difficulty in the estimation of pro-B cells, defined as HSA$^+$B220^{dull}CD43^{dull}BP-1$^-$ cells (see Fig. 2 B). Although the nature of Ig$^+$HSA$^+$ B220^{dull}CD43^{dull} cells remains unknown at present, these cells were barely detectable in the BM of N-17-95 TG and LM (data not shown).

As depicted in Fig. 7 C and summarized in Fig. 7 D, the number of BP-1$^-$ pre-B and immature B cells was comparable between Bcl-2 TG (Fig. 7, C, d and h, and D, d) and LM (Fig. 7, C, a and e, and D, a), as reported previously (39). The number of BP-1$^-$ pre-B cells was significantly reduced in N-17-95 TG (Fig. 7, C and D, b), whereas coexpression of Bcl-2 restored the number from 13 to 55% of that in LM, on average (Fig. 7, C and D, c). The number of pre-BCR$^+$ cells in BP-1$^+$ and BP-1$^-$ pre-B cells was almost comparable between Bcl-2/N-17-95 double TG and N-17-95 TG (data not shown), supporting the notion that coexpression of Bcl-2 did not affect the accumulation of

pre-B cells at the early stage. The number of immature B cells in Bcl-2/N-17-95 double TG (Fig. 7, C, g, and D, c) was approximately twofold above the level in N-17-95 TG (Fig. 7, C, f, and D, b); this effect was statistically significant ($P < 0.05$). Taken together, these results suggest the possibility that overexpression of Bcl-2 in N-17-95 TG may alleviate the reduction in the number of pre-B cells capable of progression to immature B cells.

Maximal induction of *IgL* rearrangement occurs at the late pre-B cell stage (14). The IgL rearrangement is preceded by an activation of the chromatin structure in the *IgL* locus sufficient for substrate accessibility, which is probably mediated by signaling through the pre-BCR (12–14). To delineate the maturation stage of pre-B cells in Bcl-2/N-17-95 double TG, we analyzed genomic DNA samples from purified pre-B cells by a semiquantitative PCR to measure the relative level of Igκ recombination events. As depicted in Fig. 8, there was no large difference in the relative level of Vκ joining, involving Jκ1, Jκ2, and Jκ4, in pre-B cells that were purified from the BM of N-17-95 TG, Bcl-2 TG, Bcl-2/N-17-95 double TG, and LM. Although semiquantitation of rearranged *Igκ* gene by PCR does not appear to be very sensitive, these results seem compatible with the notion that expression of Asn-17 *Ha-ras* in pre-B cells could not much affect the process of *IgL* rearrangement, and that an overexpression of Bcl-2 in N-17-95 TG restored pre-B cells undergoing *IgL* rearrangement to a considerable extent. In this regard, however, it has been previously observed that introduction of the activated form of *Ha-ras* into H chain–deficient mice resulted in an accumulation of peripheral B cells that displayed rearrangement of the *Igκ* locus (28). These results, taken together, seem compatible with the idea that $p21^{ras}$ mediates progression of B cell differentiation to a stage that is accessible to the machinery for *IgL* rearrangement, although the activity of $p21^{ras}$ is redundant in function with that of other signaling molecules at the pre-B transition. Therefore, further analysis is needed to clarify this issue.

These studies demonstrate that $p21^{ras}$ is essential for the late pre-B transition and support a role for $p21^{ras}$ in pro-B cell development (26). Thus, $p21^{ras}$ could be involved in signaling cascades that control B cell differentiation at different critical points in the BM, whereas it might not be essential for proliferation of cells at the pro-B to pre-B transition. Ras controls multiple signaling pathways (24), and activation of Raf-1 may have an important role in early B cell development in the BM (26); however, Ras-mediated signaling cascades responsible for the late pre-B transition remain to be specified. Mice disrupted with the p85α subunit of PI-3K displayed B cell deficiency, characteristics of decreased numbers of pre-B cells, and increased numbers of apoptotic cells in cultured B cells (19, 20). Because PI-3K is a direct effector of active Ras (40), the similar B cell deficit in the $p85\alpha^{-/-}$ mice and Asn-17 *Ha-ras* TG led us to speculate that inhibition of PI-3K activation could be a component of the late pre-B deficiency imposed by inhibition of $p21^{ras}$ activity.

These studies suggest that $p21^{ras}$ activity could be associated with pre-B cell survival, at least in part through regulation of Bcl-xL expression. Expression of constitutively active *Ha-ras* does not cause upregulation of *bcl-x* transcript in RAG-1–deficient B lineage cells (27), suggesting that $p21^{Ha\text{-}ras}$ may not transduce the signal for direct activation of *bcl-x* at the pro-B stage. Therefore, we speculate that $p21^{ras}$ may modulate the expression of *bcl-x* in concert with other signaling molecules. Consistent with $p21^{ras}$ activity for pre-B cell survival, overexpression of the antiapoptotic protein Bcl-2 alleviated the reduction in the number of late pre-B cells in Asn-17 *Ha-ras* transgenic animals, but it did not restore the number of cells to the normal level. Considering that cell survival is regulated by the Bcl-2 member of proteins that consists of anti- and proapoptotic members (for reviews, see references 38 and 41), the results might imply that $p21^{ras}$ provides multiple effector pathways for pre-B cell survival, in addition to regulation of antiapoptotic activity. In this context, it has previously been suggested that $p21^{ras}$ activates Akt/protein kinase B (PKB) kinase via PI-3K and ERK via Raf-1, which control the activity of proapoptotic effects in different types of cells in vitro (for a review, see reference 42). Antiapoptotic molecules may function by inhibiting the process of caspase activation, whereas proapoptotic proteins may independently regulate a common apoptotic pathway or function by heterodimerization with antiapoptotic proteins (38, 41). Therefore, it is conceivable that exogenous Bcl-2 activity in Asn-17 *Ha-ras* TG would be overridden by proapoptotic activity, which could be downregulated by $p21^{ras}$ in pre-B cells in a normal state. Whether $p21^{ras}$ regulates pre-B cell survival through multiple effector pathways remains to be elucidated.

We are grateful to Dr. Hirofumi Nishizumi (University of Tokyo) for his critical review of the manuscript, Drs. G.M. Cooper (Dana-Farber Cancer Institute) and Y. Nakafuku (Nara Institute of Science and Technology, Japan) for reagents, and to Ms. K. Nakano and M. Takizawa for operation of the FACS®.

This work was supported by a grant from the Agency of Technology and Science of the Japanese government to T. Takemori.

Submitted: 25 August 1999
Revised: 20 March 2000
Accepted: 18 May 2000

References

1. Karasuyama, H., A. Rolink, and F. Melchers. 1996. Surrogate light chain in B cell development. *Adv. Immunol.* 63:1–41.
2. Li, Y.-S., K. Hayakawa, and R.R. Hardy. 1993. The regulated expression of B lineage–associated genes during B cell differentiation in bone marrow and fetal liver. *J. Exp. Med.* 178:951–960.
3. Li, Y.-S., R. Wasserman, K. Hayakawa, and R.R. Hardy. 1996. Identification of the earliest B lineage stage in mouse bone marrow. *Immunity*. 5:527–535.
4. Kitamura, D., and K. Rajewsky. 1992. Targeted disruption of μ membrane exon causes loss of heavy chain allelic exclusion. *Nature*. 356:154–156.
5. Kitamura, D., A. Kudo, S. Schaal, W. Mueller, F. Melchers,

and K. Rajewsky. 1992. A critical role of λ5 protein in B cell development. *Cell*. 69:823–831.
6. Papavasiliou, F., Z. Misulovin, H. Suh, and M.C. Nussenzweig. 1995. The role of Igα in precursor B cell transition and allelic exclusion. *Science*. 268:408–411.
7. Papavasiliou, F., M. Jankovie, H. Suh, and M.C. Nussenzweig. 1995. The cytoplasmic domains of immunoglobulin (Ig)α and Igβ can independently induce the precursor B cell transition and allelic exclusion. *J. Exp. Med*. 182:1389–1394.
8. Torres, R.M., H. Flaswinkel, M. Reth, and K. Rajewsky. 1996. Aberrant B cell development and immune response in mice with a compromised BCR complex. *Science*. 272:1804–1808.
9. Motoyama, N., F. Wang, K.A. Roth, H. Sawa, K.-I. Nakayama, K. Nakayama, I. Negishi, S. Senju, Q. Zhang, S. Fuji, and D.Y. Lo. 1995. Massive cell death of immature hematopoietic cells and neurons in Bcl-x-deficient mice. *Science*. 267:1506–1510.
10. Fang, W., D.L. Mueller, C.A. Pennell, J.J. Rivard, Y.-S. Li, R.R. Hardy, M.S. Schlissel, and T.W. Behrens. 1996. Frequent aberrant immunoglobulin gene rearrangement in pro-B cells revealed by bcl-xL transgene. *Immunity*. 4:291–299.
11. Grillot, D.A.M., R. Merino, J.C. Pena, W.C. Fanslow, F.D. Finkelman, and C.B. Thompson, and G. Nunez. 1996. Bcl-x exhibits regulated expression during B cell development and activation and modulates lymphocyte survival in transgenic mice. *J. Exp. Med*. 183:381–391.
12. Reth, M., E. Petrac, P. Wiese, L. Lobel, and F.W. Alt. 1987. Activation of V kappa gene rearrangement in pre-B cells follows the expression of membrane-bound immunoglobulin heavy chains. *EMBO (Eur. Mol. Biol. Organ.) J.* 6:3299–3305.
13. Nussenzweig, M.C., A.C. Shaw, E. Sinn, D.B. Danner, K.L. Holmes, H.C. Morse, and P. Leder. 1987. Allelic exclusion in transgenic mice that express the membrane form of immunoglobulin μ chains. *Science*. 236:816–819.
14. Constantinescu, A., and M.S. Schlissel. 1997. Changes in locus-specific V(D)J recombinase activity induced by immunoglobulin gene products during B cell development. *J. Exp. Med*. 185:609–620.
15. Reth, M. 1989. Antigen receptor tail clue. *Nature*. 338:383–384.
16. Kurosaki, T. 1999. Genetic analysis of B cell antigen receptor signaling. *Annu. Rev. Immunol*. 17:555–592.
17. Turner, M., P.J. Mee, P.S. Costello, O. Williams, A.A. Price, L.P. Duddy, M.T. Furlong, R.L. Geahlen, and V.L. Tybulewicz. 1995. Perinatal lethality and blocked B-cell development in mice lacking the tyrosine kinase Syk. *Nature*. 378: 298–302.
18. Cheng, A.M., B. Rowley, W. Pao, A. Hayday, J.B. Bolen, and T. Pawson. 1995. Syk tyrosine kinase required for mouse viability and B-cell development. *Nature*. 378:303–306.
19. Suzuki, H., Y. Terauchi, M. Fujiwara, S. Aizawa, Y. Yazaki, T. Kadowaki, and S. Koyasu. 1999. Xid-like immunodeficiency in mice with disruption of the p85α subunit of phosphoinositide 3-kinase. *Science*. 283:390–392.
20. Fruman, D.A., S.B. Snapper, C.M. Yballe, L. Davidson, J.Y. Yu, F.W. Alt, and L.C. Cantley. 1999. Impaired B cell development and proliferation in absence of phosphoinositide 3-kinase p85α. *Science*. 283:393–397.
21. Pappu, R., A.M. Cheng, B. Li, Q. Gong, C. Chiu, N. Griffin, M. White, B.P. Sleckman, and A.C. Chan. 1999. Requirement for B cell linker protein (BLNK) in B cell development. *Science*. 286:1949–1954.
22. Minegishi, Y., J. Rohrer, E. Coustan-Smith, H.M. Lederman, R. Pappu, D. Campana, A.C. Chan, and M.E. Conley. 1999. An essential role for BLNK in human B cell development. *Science*. 286:1954–1957.
23. Jamma, H., B. Wollscheid, M. Mitterer, J. Wienands, M. Reth, and P.J. Nielsen. 1999. Abnormal development and function of B lymphocytes in mice deficient for the signaling adapter protein SLP-65. *Immunity*. 11:547–554.
24. Rommel, C., and E. Hafen. 1998. Ras—a versatile cellular switch. *Curr. Opin. Genet. Dev*. 8:412–418.
25. Feig, L.A., and G.M. Cooper. 1988. Inhibition of NIH3T3 cell proliferation by a mutant ras protein with preferential affinity for GDP. *Mol. Cell Biol*. 8:3235–3243.
26. Iritani, B.M., K.A. Forbush, M.A. Farra, and R.M. Perlmutter. 1997. Control of B cell development by Ras-mediated activation of Raf. *EMBO (Eur. Mol. Biol. Organ.) J.* 16:7019–7031.
27. Shaw, A.C., W. Swat, R. Ferrini, L. Davidson, and F.W. Alt. 1999. Activated Ras signals developmental progression of recombinase-activating gene (RAG)-deficient pro-B lymphocytes. *J. Exp. Med*. 189:123–129.
28. Shaw, A.C., W. Swat, L. Davidson, and F.W. Alt. 1999. Induction of Ig light chain gene rearrangement in heavy chain-deficient B cells by activated Ras. *Proc. Natl. Acad. Sci. USA*. 96:2239–2243.
29. Meyer, K.B., Y.-M. Teh, and M.S. Neuberger. 1996. The Igκ 3′-enhancer triggers gene expression in early B lymphocytes but its activity is enhanced on B cell activation. *Int. Immunol*. 8:1561–1568.
30. Kimoto, H., H. Nagaoka, Y. Adachi, T. Mizuochi, T. Azuma, T. Yagi, T. Sata, S. Yonehara, Y. Tsunetsugu-Yokota, M. Taniguchi, and T. Takemori. 1997. Accumulation of somatic hypermutation and antigen-driven selection in rapidly cycling surface Ig^+ germinal center (GC) B cells which occupy GC at high frequency during the primary antihapten response in mice. *Eur. J. Immunol*. 27:268–279.
31. Winkler, T.H., A. Rolink, F. Melchers, and H. Karasuyama. 1995. Precursor B cells of mouse bone marrow express two different complexes with two surrogate light chains on the surface. *Eur. J. Immunol*. 25:446–450.
32. Kashiwada, M., Y. Shirakata, J.-I. Inoue, H. Nakano, K. Okazaki, K. Okumura, T. Yamamoto, H. Nagaoka, and T. Takemori. 1998. Tumor necrosis factor receptor–associated factor 6 (TRAF6) stimulates extracellular signal–regulated kinase (ERK) activity in CD40 signaling along a Ras-independent pathway. *J. Exp. Med*. 187:237–244.
33. Hayashi, R., T. Takemori, M. Kodama, M. Suzuki, A. Tsuboi, F. Nagawa, and H. Sakano. 1997. The PU.1 binding site is a cis-element that regulates pro-B/pre-B specificity of Vκ-Jκ joining. *J. Immunol*. 159:4145–4149.
34. Cooper, M.D., D. Mulvaney, A. Coutinho, and P.-A. Cazenave. 1986. A novel cell surface molecule on early B-lineage cells. *Nature*. 321:616–618.
35. Karasuyama, H., A. Rollink, Y. Shinkai, F. Young, F.W. Alt, and F. Melchers. 1994. The expression of Vpre-B/λ5 surrogate light chain in early bone marrow precursor B cells of normal and B cell-deficient mutant mice. *Cell*. 77:133–143.
36. Osmond, D.G. 1990. B cell development in the bone marrow. *Semin. Immunol*. 2:173–180.
37. Nagata, K., T. Nakamura, F. Kitamura, S. Kuramochi, S. Taki, K.S. Campbell, and H. Karasuyama. 1997. The Igα/Igβ heterodimer on μ-negative proB cells is competent for transduction signals to induce early B cell differentiation. *Im-*

munity. 7:559–570.
38. Chao, D.T., and S.J. Korsmeyer. 1998. Bcl-2 family: regulators of cell death. *Annu. Rev. Immunol*. 16:395–419.
39. Merino, R., L. Ding, D.J. Veis, S.J. Korsmeyer, and G. Nunez. 1994. Developmental regulation of the Bcl-2 protein and susceptibility to cell death in B lymphocytes. *EMBO (Eur. Mol. Biol. Organ.) J.* 13:683–691.
40. Rodriguez-Viciana, P., P.H. Waren, R. Dhand, B. Vanhaesebroeck, I. Gout, M.J. Fry, M.D. Waterfield, and J. Downward. 1994. Phosphatidylinositol-3-OH kinase as a direct target of Ras. *Nature*. 370:527–532.
41. Adams, J.M., and S. Cory. 1998. The Bcl-2 protein family: arbiters of cell survival. *Science*. 281:1322–1326.
42. Downward, J. 1998. Ras signalling and apoptosis. *Curr. Opin. Genet. Dev*. 8:49–54.